Amino Acids (2014) 46:2463–2475
DOI 10.1007/s00726-014-1808-x

ORIGINAL ARTICLE

Transport mechanism and regulatory properties of the human amino acid transporter ASCT2 (SLC1A5)

Mariafrancesca Scalise · Lorena Pochini · Simona Panni · Piero Pingitore · Kristina Hedfalk · Cesare Indiveri

Received: 9 April 2014 / Accepted: 6 July 2014 / Published online: 23 July 2014

Abstract The kinetic mechanism of the transport catalyzed by the human glutamine/neutral amino acid transporter hASCT2 over-expressed in *P. pastoris* was determined in proteoliposomes by pseudo-bi-substrate kinetic analysis of the Na^+-glutamine$_{ex}$/glutamine$_{in}$ transport reaction. A random simultaneous mechanism resulted from the experimental analysis. Purified functional hASCT2 was chemically cross-linked to a stable dimeric form. The oligomeric structure correlated well with the kinetic mechanism of transport. Half-saturation constants (Km) of the transporter for the other substrates Ala, Ser, Asn and Thr were measured both on the external and internal side. External Km were much lower than the internal ones confirming the asymmetry of the transporter. The electric nature of the transport reaction was determined imposing a negative inside membrane potential generated by K^+ gradients in the presence of valinomycin. The transport reaction resulted to be electrogenic and the electrogenicity originated from external Na^+. Internal Na^+ exerted a stimulatory effect on the transport activity which could be explained by a regulatory, not a counter-transport, effect. Native and deglycosylated hASCT2 extracted from HeLa showed the same transport features demonstrating that the glycosyl moiety has no role in transport function. Both in vitro and in vivo interactions of hASCT2 with the scaffold protein PDZK1 were revealed.

Keywords Amino acid · Glutamine · Plasma membrane · Transport · Liposomes · Scaffold protein

Abbreviations

$C_{12}E_8$	Octaethylene glycol monododecyl ether
YPDS	Yeast Extract Peptone Dextrose Sorbitol
BMGY	Buffered Glycerol-complex Medium
DOC	Na-deoxycholate
NP-40	Nonidet
MeAIB	A-(methylamino)isobutyric acid
BCH 2-aminobicyclo	(2,2,1)-heptane-2-carboxylic acid

Introduction

The human plasma membrane transporter SLC1A5, previously named ASCT2, catalyzes transport of neutral amino acids. In spite of the original acronym AlaSerCys Transporter 2, the amino acid which underlies the special roles of this transporter in human physiology and pathology is glutamine. ASCT2 is ubiquitously expressed and, hence, it is responsible for glutamine disposition to several tissues, contributing, as example, to the maintenance of nitrogen homeostasis which is particularly important in nervous tissue (Adeva et al. 2012; Bode 2001). Recently, an important role of ASCT2 in cancer development and progression emerged. The transporter, together with the large amino acid Transporter 1, LAT1 (SLC7A5), has been found over-expressed in several cancers (Fuchs and Bode

M. Scalise · L. Pochini · S. Panni · P. Pingitore · C. Indiveri (✉)
Department DiBEST (Biologia, Ecologia, Scienze della Terra) Unit of Biochemistry and Molecular Biotechnology, University of Calabria, Via P. Bucci 4C, 87036 Arcavacata di Rende, CS, Italy
e-mail: cesare.indiveri@unical.it

K. Hedfalk
Department of Chemistry and Molecular Biology, University of Gothenburg, PO Box 462, SE-405 30 Goteborg, Sweden

2005; Shimizu et al. 2014). This phenomenon relies on the typical metabolic features of cancer cells, collectively known as Warburg effect (Broer 2011; Ganapathy et al. 2009). Cancer cells, in fact, require high amounts of glutamine for energy and growth purposes through a complex pathway involving glutaminolysis and a truncated form of the citric acid cycle. This network supplies carbon atoms both as source of ATP synthesis, at the substrate level, and of NADPH for reductive biosynthesis (Fuchs and Bode 2005; Ganapathy et al. 2009). Moreover, ASCT2 is linked to mTOR signaling which is particularly sensitive to intracellular L-glutamine and L-asparagine (Fuchs et al. 2007; Nicklin et al. 2009). Deprivation of these amino acids induces mTOR activated autophagy. The link to ASCT2 expression has been recently demonstrated: upon silencing ASCT2 gene in hepatoma cells, mTOR activates cell growth repression triggering apoptosis (Fuchs and Bode 2005; Fuchs et al. 2007; Nicklin et al. 2009). All these features make the ASCT2 transporter object of hot research topics. This protein has been, in fact, proposed as target for anticancer therapy (Albers et al. 2012; Oppedisano et al. 2012; Shimizu et al. 2014). While structural information on ASCT2 is missing due to the challenges in obtaining crystals of this protein (Indiveri et al. 2013), several functional studies on the murine and human isoforms, have been conducted so far, both in cell systems (Utsunomiya-Tate et al. 1996; Torres-Zamorano et al. 1998; Broer et al. 1999, 2000) and in proteoliposomes (Oppedisano et al. 2004, 2007; Pingitore et al. 2013). This tool was previously used for studying the rat isoform of ASCT2 extracted from kidney, which has been extensively characterized on physiological, toxicological and pharmacological aspects (Oppedisano et al. 2004, 2007, 2010, 2012). Very recently, the human isoform of ASCT2 has been heterologously over-expressed and purified in large scale from the methylotrophic yeast *P. pastoris* (Pingitore et al. 2013). Similarly to the rat isoform, hASCT2 has been reconstituted in proteoliposomes. The basic functional properties have been studied and found to be very similar to those previously described in cell systems: the transporter catalyzes an obligatory antiport of glutamine and other neutral amino acids, strictly dependent on external Na^+, which cannot be substituted by other cations (Pingitore et al. 2013). Moreover, new functional aspects of the human isoform were shown, such as the asymmetry in substrate recognition and transport, which was not yet revealed in cell systems. The amino acids glutamine, asparagine, serine and threonine can be transported either inwardly or outwardly. On the contrary, alanine, methionine and valine can be only inwardly transported (Pingitore et al. 2013). However, some important information on hASCT2 is still lacking or controversial, such as the kinetic mechanism, the electrical aspects of the antiport reaction and, in general, the regulatory properties. Some previous reports described murine ASCT2 as an electroneutral exchanger of both neutral amino acids and Na^+ (Utsunomiya-Tate et al. 1996; Broer et al. 2000). This issue was further exploited. The rat ASCT2 has been proposed as an electrogenic antiporter on the basis of experimental and computational approaches (Zander et al. 2013). Clarifying and completing the knowledge, especially of the human (h)ASCT2, is of great importance for understanding the biological functions of this transporter and, hence, its involvement in human pathology. This is particularly relevant since the identity between the human and rat ASCT2 is lower than the identity normally found in the case of other transporters (Broer et al. 1999; Oppedisano et al. 2011; Indiveri et al. 2013). These aspects are fundamental for planning pharmacological interventions devoted to prevent cancer progression. In the present work, the proteoliposome tool, recently pointed out for the recombinant human transporter, in combination with other experimental strategies, allowed us to clarify and to obtain several new data on the hASCT2. The transport mechanism of the ter-reactant reaction ($glutamine_{ex}$-Na^+_{ex}/$glutamine_{in}$) and the electrical properties of the Na^+-coupled transport were assessed. The role of Na^+ in regulating the transport function has been clarified: external Na^+ is involved in transport and is responsible for the electrogenicity, while internal Na^+ is not a transported modulator of the reaction. Moreover, it was assessed that the glycosyl moiety is not involved in transport function. The novel interaction of ASCT2 with the scaffold protein PDZK1 was described.

Materials and methods

Materials

The *P. pastoris* wild type strain (X-33), Ni–NTA agarose, DMEM, Fetal Calf serum, antibiotics and reagents for cancer cell line were from Invitrogen; PD-10 columns, ECL plus, Hybond ECL membranes, Gluthatione-Sepharose 4B resin from GE Healthcare; L-[^{3}H]glutamine, L-[^{3}H]serine, were from Perkin Elmer; L-[^{3}H]alanine, L-[^{3}H]threnonine and L-[^{3}H]asparagine were from ARC (American Radioladiolabeled Chemicals); the anti-rabbit IgG HRP conjugate from cell signaling; the anti-hASCT2 from Millipore; HeLa cells were from ATCC; protease inhibitor tablets were from Roche; *E.coli* BL21 Rosetta strain was used to express GST and His fusion proteins; Bio-rad protein assay was from Biorad; anti-His_6 antibody, $C_{12}E_8$, Amberlite XAD-4, egg yolk phospholipids (3-sn-phosphatidylcoline from egg yolk), Sephadex G-75, L-glutamine, valinomycin and all the other reagents were from Sigma-Aldrich.

Recombinant production of hASCT2

For large-scale hASCT2 production, *P. pastoris* strain X-33, was transformed with pPICZB-hASCT2-His_6 optimized according to genomic host codon usage as previously described (Pingitore et al. 2013). The *P. pastoris* strains were grown at 30 °C in a 3 L fermentor (Infors HT) having an Initial Fermentation Volume (IFV) of 1.5 L as previously described (Pingitore et al. 2013). To induce production of recombinant hASCT2, the culture was fed with 150 mL methanol for 48 h. To obtain the membrane fraction, *P. pastoris* cells overproducing hASCT2 were resuspended in a buffer containing 50 mM Tris, pH 7.4, 150 mM NaCl, 6 mM β-mercaptoethanol and 0.5 mM PMSF at a concentration of about 1 g/mL. Droplets of the cell suspension were frozen in liquid nitrogen and cells broken by an X-Press (four passages). The suspension was treated as described previously to recover membrane fractions (Pingitore et al. 2013). The washed membrane fractions (pellet) containing hASCT2 were resuspended in a buffer containing 25 mM Tris, pH 7.4, 250 mM NaCl, 6 mM β-mercaptoethanol and 10 % glycerol at a final concentration of about 300 mg/mL and homogenized using a hand-held electric homogenizer.

Solubilization and purification of hASCT2

For large-scale solubilization and purification hASCT2-His_6, about 1.5 g of washed membranes (300 mg/mL) was resuspended in the same buffer described above added with 1 % $C_{12}E_8$ (w/w) and gently mixed by agitation for 3 h at 4 °C. The solubilized material was centrifuged at 120,000 g for 1 h and applied to 3 mL Ni-nitrilotriacetic acid agarose resin for Nickel chelating chromatography as previously described (Pingitore et al. 2013). The elution of recombinant protein was performed by imidazole gradient followed by passage on PD-10 desalting column (equilibrated with 70 mM NaCl and Tris/HCl 20 mM pH 7.0).

Reconstitution of the recombinant hASCT2 into liposomes

The purified hASCT2 was reconstituted by removing the detergent using the batch-wise method (Pingitore et al. 2013). In this procedure, the mixed micelles containing detergent, protein and phospholipids, prepared as previously described (Scalise et al. 2013), were incubated with 0.5 g Amberlite XAD-4 resin under rotatory stirring (1,200 rev/min) at room temperature (25 °C) for 40 min (Pochini et al. 2012). The composition of the initial mixture used for reconstitution was: 100 µL of the solubilized protein (5 µg protein in 70 mM NaCl and Tris/HCl 20 mM pH 7.0), 120 µL of 10 % $C_{12}E_8$, 100 µL of 10 % egg yolk phospholipids (w/v) in the form of sonicated liposomes, 10 mM L-glutamine (except where differently specified) and 20 mM Tris/HCl pH 7.0 in a final volume of 700 µL (Pingitore et al. 2013). All the operations were performed at 4 °C. Reshuffling of proteoliposomes was obtained by three repeated cycles of freeze in liquid N_2 and slow thawing at 0 °C followed by pulse sonication (2 s sonication 2 s intermission, at 35 W) (Indiveri et al. 1991).

Reconstitution of hASCT2 extracted from HeLa cells

HeLa cells (cervical cancer-derived cell line) were cultured using standard culturing conditions. hASCT2 was solubilized from cell membrane by using RIPA buffer (150 mM NaCl, 20 mM Tris–HCl pH 7.4, 1 mM ethylenediaminetetraacetic acid, 1 mM ethylene glycol tetraacetic acid), 1 % NP-40, 1 % sodium deoxycholate, supplemented with protease inhibitor tablet. Protein concentration was determined by Lowry method using Bovine Serum Albumin (BSA) as standard. After quantification, 30 µg of total extract was reconstituted in liposomes as reported above for recombinant hASCT2 and transport measurement was performed as described in the paragraph "Transport measurement". The HeLa extract was used for deglycosylation experiment according to manufacturer's protocol (protein deglycosylation mix from NEB, P6039S). Protein samples were analyzed on SDS-PAGE 12 % and transferred onto nitrocellulose membranes. Western blot analysis was performed using anti-hASCT2 1:2000 (rabbit, Millipore) incubated over night in 3 % BSA under shaking at 4 °C and revealed by chemiluminescence. The transport activity of deglycosylated protein was assayed after proteoliposomes reconstitution as described before.

Transport measurements

To remove the external substrate, 600 µL of proteoliposomes was passed through a Sephadex G-75 column (0.7 cm diameter × 15 cm height) pre-equilibrated with 20 mM Tris/HCl pH 7.0 and sucrose at an appropriate concentration to balance the internal osmolarity. Transport measurement, performed at 25 °C, was started by adding 50 µM [^{3}H] glutamine and 50 mM Na-gluconate (except where differently specified) to the proteoliposomes; the transport was stopped by adding 10 µM $HgCl_2$ at the desired time interval according to the stop inhibitor method, as previously described (Pingitore et al. 2013). The initial rate of transport was measured by stopping the reaction after 10 min, i.e., within the initial linear range of [^{3}H] glutamine uptake into the proteoliposomes as previously reported (Pingitore et al. 2013). At the end of the transport assay, each sample of proteoliposomes (100 µL) was passed through a Sephadex G-75 column (0.6 cm diameter × 8 cm height) to separate the external from the

internal radioactivity. Liposomes were eluted with 1 mL 50 mM NaCl and collected in 4 mL of scintillation mixture, vortexed and counted. Experimental data were fitted in a first-order rate equation to obtain rate constants and in Michaelis–Menten, Linewever-Burk or Headie-Hofstee equation using non-linear fitting analysis by Grafit software (version 5.0.13).

To measure the specific activity of hASCT2, the mg protein (referred to as mg through the manuscript) was estimated from Coomassie blue stained SDS-PAGE gels by using the Chemidoc imaging system equipped with Quantity One software (Bio-Rad) as previously described (Giancaspero et al. 2013).

To generate K^+ diffusion potential, 50 mM K-gluconate was added to the reconstitution mixture in the presence of 0.5 mM external K-gluconate (except when differently specified) to reach a membrane potential of −120 mV according to Nernst's equation. Valinomycin (0.75 µg/mg phospholipid) in ethanol was added to the proteoliposomes as previously described (Oppedisano et al. 2011).

Kinetics

For the determination of the kinetic mechanism, analyses of pseudo-bi-reactant transport reactions were performed measuring the transport rate as a function of concentrations of two (pseudo-substrate 1 and 2) out of three substrates, keeping constant the third one. Data were analyzed in Lineweaver–Burk plots. The equation used is:

$$\frac{1}{V} = \frac{1}{V_{\max}} + K_{S1}/(V_{\max} \times S1) + K_{S2}/(V_{\max} \times S2) + K_{iS1} \times K_{S2}/(V_{\max} \times S1 \times S2)$$

where: S1, concentration of the first pseudo-substrate; S2, concentration of the second pseudo-substrate; K_{iG}, dissociation constant for the binary transporter-Gln complex; $K_{S1,}$ dissociation constant (Km) of the first substrates for the ternary transporter-S1-S2 complex; K_{S2}, dissociation constant (Km) of S2 for the ternary transporter-S2-S1 complex. K_{iS2}, can be introduced by simply transcribing the equation for S2 as the variable substrate. In a random sequential mechanism $K_{iS1} \times K_{S2} = K_{iS2} \times K_{S1}$ (Cleland 1970).

Pulldown experiments

Human PDZK1 was cloned in pGEX2T vector and expressed in *E. coli* BL21 Rosetta as GST fusion protein. The protein was affinity purified from the extracts onto gluthatione-Sepharose 4B resin, and quantified with Bio-rad protein assay. The C- terminal fragment of human ASCT2 (aa 447-541) was cloned in pET-28a(+) and expressed in *E. coli* BL21 Rosetta as recombinant protein with the N-terminal extra-sequence hhhhhhssglvprgshmasmtggqqmgrgdefelr deriving from the plasmid and containing a His_6 tag. For pull-down experiment, bacterial extracts expressing hASCT2 were incubated with 50 µg of PDZK1-GST or with 50 µg of GST alone as a control bound to Gluthatione-Sepharose beads. After 2 h at 4 °C the resins were washed repeatedtly in a buffer containing PBS and 0.05 % tween 20. The bound proteins were recovered by boiling in 50 mM Tris pH 6.8, 100 mM dithiothreitol, 2 % SDS, 1 % bromophenol blue, 10 % glycerol. Samples were analyzed on a 17 % SDS-PAGE gel and transferred onto nitrocellulose membranes. Western blot analysis was performed using anti-His POD conjugated (1:10000) incubated 1 h in 3 % BSA under shaking at room temperature and revealed by chemiluminescence. To assess the binding with both the endogenous and over-expressed full-length proteins (see also legend to Fig. 8), HeLa cells were lysed with RIPA buffer (see above). Extracts were centrifuged for 15 min at 14.000 rpm 4 °C and the supernatant was incubated with resin-bound PDZK1-GST as above described. Western blot analysis has been performed using anti- ASCT2 antibody 1:2,000 incubated over night in 3 % BSA under shaking at room temperature and revealed by chemiluminescence.

Cross-linking of hASCT2

Purified ASCT2 obtained by over-expression in *P. pastoris* has been used for cross-linking reaction with formaldehyde. The protein has been treated with increasing concentrations of cross-linker (see results and legend to Fig. 3) for 30 min at 23 °C, 700 rpm. The reaction has been stopped adding cold glycine 1 M solubilized in PBS. The samples have been analyzed on SDS-PAGE and detected by western blot analysis with anti hASCT2 1:2,000 (Millipore) incubated over night in 3 % BSA under shaking at 4 °C and revealed by chemiluminescence.

Results

Transport mechanism

The orientation of the hASCT2 transporter in proteoliposomes with the same sidedness as in cell membrane has been previously suggested on the basis of the obligatory dependence on external Na^+ and the finding of single Km values outside and inside (Pingitore et al. 2013). For a definitive proof of the sidedness, a previously pointed out procedure for proteoliposome reshuffling (Indiveri et al. 1991) was applied to hASCT2. Data were analyzed by the Eadie-Hofstee plot in which the Km is derived from the slope. After reconstitution, a single Km value was observed on the external side (Fig. 1a), which is very similar to that

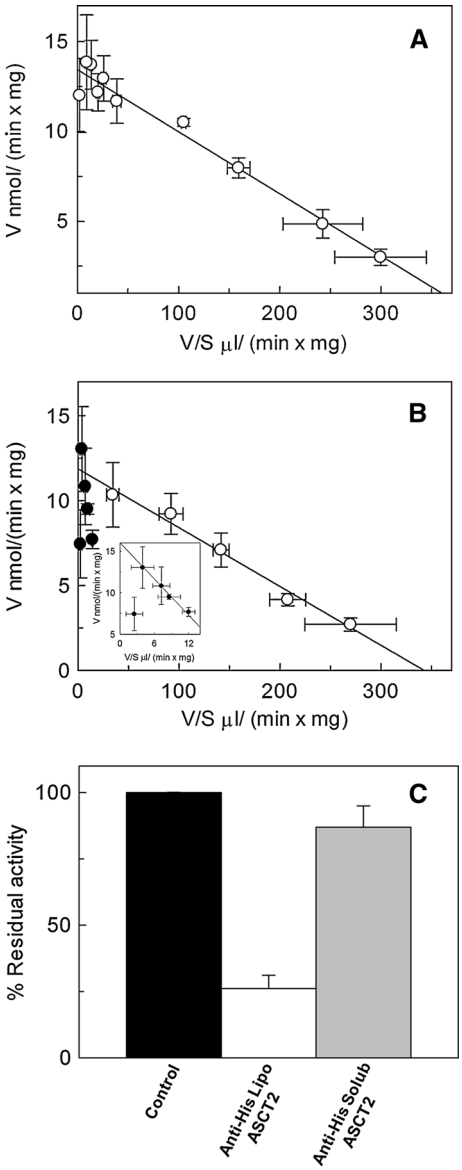

Fig. 1 Sidedness of the reconstituted hASCT2 in proteoliposomes. Km values for glutamine were measured at the external membrane side before (**a**) and after (**b**) freeze/thaw/sonication of the proteoliposomes (reshuffling). The internal glutamine concentration was 10 mM. The transport reaction was started by adding [^{3}H]glutamine at concentrations ranging from 0.01 to 5 mM in the presence of 50 mM Na-gluconate and stopped at 10 min as described in "Materials and methods". In **a** (*unfilled circle*), a single Km value was calculated, 40 µM. In **b** two different interpolation fitted the experimental points indicating the external Km, 40 µM (*unfilled circle*) or internal Km, 0.8 mM (*filled circle*). The inset in 1 b is an expanded region of black circles. The values were calculated from the slope of the Eadie-Hofstee plots. *V* initial transport rate, *S* concentration of external [^{3}H]glutamine. The values are mean ± SD from three experiments. In **c** the hASCT2 has been incubated before (*white bar*; Anti-His Solub. ASCT2) and after (*gray bar*; Anti-His Lipo ASCT2) reconstitution with anti-His antibody targeting the C-ter of the protein. The transport reaction was started by adding 50 µM [^{3}H] glutamine in the presence of 50 mM Na-gluconate and stopped after 10 min as described in "Materials and methods". The transport activity is indicated as % of residual activity respect to control without antibody (*black bar*). The values are mean ± SD from three experiments

measured by other analysis (see below) and to the Km for glutamine on the external side of cells for the human ASCT2 (Torres-Zamorano et al. 1998). After reshuffling, two Km values were measured. One, in the µM range (opened circles), which corresponded to the external Km; and the other, in the mM range (filled circles), which corresponded to the internal Km for glutamine (Fig. 1b). This unequivocally demonstrates that before reshuffling, virtually all the proteoliposomes were sided similarly to the cell membrane. However, some of the data points related to the internal Km (filled circles and inset of Fig. 1b) showed lower V values than expected; this is explained by the lower intra-liposomal Na^+ concentration compared to that required by the external face of the inverted protein (50 mM Na^+; Pingitore et al. 2013). Moreover, some substrate inhibition effects may also contribute, as it appears from data points in Fig. 1a, corresponding to higher glutamine concentrations. To further confirm the orientation of the protein, additional evidence is provided. According to the presence of a Cys residue exposed towards the extra-liposomal, i.e., extracellular side (Pingitore et al. 2013), the hydrophilic impermeant SH reagent MTSET led to nearly complete inhibition of the hASCT2 activity at 0.25 mM with an IC50 of 5 µM (not shown). Moreover, an immuno-labeling approach was used (Fig. 1c). hASCT2 carries a 6-His tag at the intracellular C-terminal which is recognized by a specific anti-His antibody (Pingitore et al. 2013). hASCT2 was incubated with the anti-His antibody before (solubilized protein) or after reconstitution in proteoliposomes. The incubation of the solubilized protein, whose C-terminal was reachable by the antibody, virtually completely inhibited hASCT2 compared to the untreated control. On the contrary, incubation of proteoliposomes with the same antibody resulted in complete protection from inhibition indicating an intra-liposomal localization of the C-terminal (Fig. 1c). Taken together, the results from Fig. 1 are in favor of full orientation of hASCT2 in proteoliposomes as in cell membrane. The kinetic mechanism of the ter-reactant Na^+-glutamine$_{ex}$/glutamine$_{in}$ antiport was analyzed by a pseudo-bi-reactant kinetic analysis, in which the concentration of one of the three substrates was kept, alternatively, constant (close to saturation) and the concentrations of the others were varied (Indiveri et al. 2001). In particular, transport rate was measured as [^{3}H]-glutamine uptake in proteoliposomes containing 10 mM glutamine, as function of the external glutamine (Fig. 2a), or Na-gluconate (Na^+) (Fig. 2b) concentrations. Moreover, the rate of [^{3}H]-glutamine uptake was measured as function of the external (Fig. 2c) or internal glutamine (Fig. 2d) concentrations, keeping constant the concentration of external Na^+. The experimental data were plotted according to Lineweaver–Burk, as reciprocal transport rate vs reciprocal substrate concentration. This representation allows to discriminate

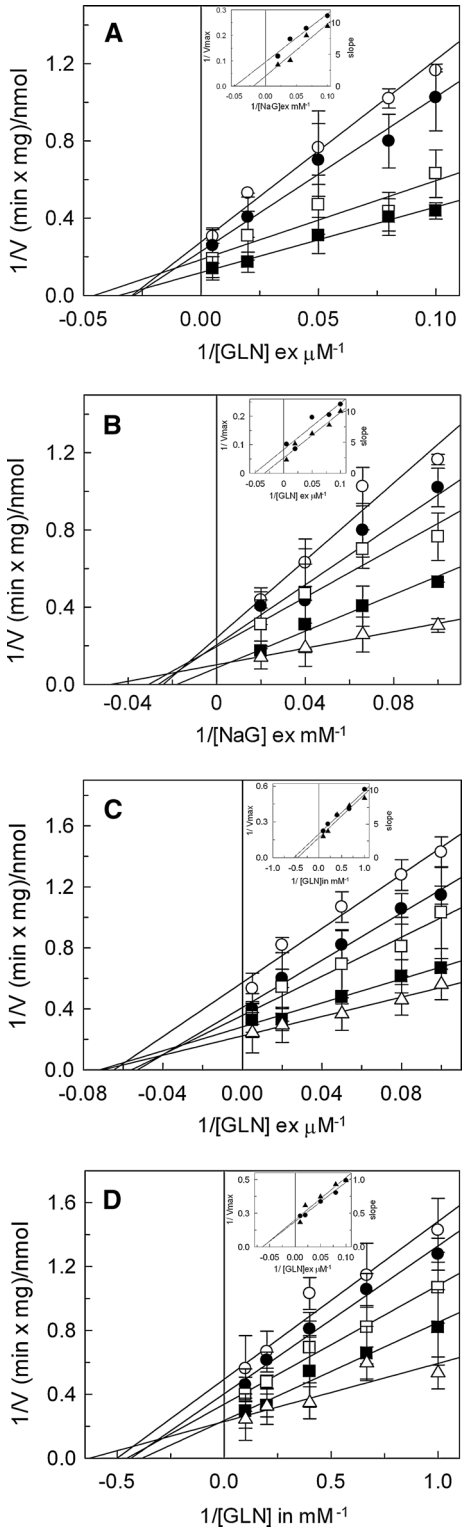

Fig. 2 Mechanism of the Na^+-glutamine$_{ex}$/glutamine$_{in}$ transport reaction mediated by hASCT2 in proteoliposomes. Lineweaver–Burk plots showing the dependence of reciprocal transport rate on reciprocal external glutamine (**a**) or Na-gluconate (**b**) concentrations at constant (10 mM) intraliposomal glutamine concentration. Transport reaction was stopped at 10 min as described in "Materials and methods". In **a** the concentrations of Na-gluconate were 10 (*unfilled circle*), 15 (*filled circle*), 25 (*unfilled square*) and 50 (*filled circle*) mM. In **b** the concentrations of [^{3}H]glutamine were 10 (*unfilled circle*), 12.5 (*filled circle*), 20 (*unfilled square*), 50 (*filled circle*) and 200 (*unfilled triangle*) μM. Lineweaver–Burk plots showing the dependence of reciprocal transport rate on reciprocal external (**c**) or internal glutamine (**d**) concentrations at constant (50 mM) extraliposomal Na-gluconate concentration. In **c** the concentrations of external [^{3}H]glutamine were 10 (*unfilled circle*), 12.5 (*filled circle*), 20 (*unfilled square*), 50 (*filled square*) and 200 (*unfilled triangle*) μM. In **d** the concentrations of internal glutamine were 1 (*unfilled circle*), 1.5 (*filled circle*), 2.5 (*unfilled square*), 5 (*filled square*) and 10 (*unfilled triangle*) mM. In each figure an inset with secondary plots obtained by re-plotting the values of the intercepts on the *Y*-axis ($1/V_{max}$ *filled circle*) or the slopes (*filled triangle*) of the straight lines from the primary plots as a function of external Na-gluconate (**a**), external glutamine (**b**, **d**) and internal glutamine (**c**) concentrations. The values are mean ± SD from three experiments

between ping-pong and simultaneous mechanisms which result, respectively, in parallel and non-parallel patterns of straight lines. In all the analyzed reactions (Fig. 2), the straight lines showed non-parallel patterns intersecting in proximity of the X-axis. These data demonstrated that the overall Na^+-glutamine$_{ex}$/glutamine$_{in}$ transport reaction follows a simultaneous mechanism. This mechanism can be further differentiated in two sub-types: (i) random, which occurs when the two substrates do not have any preferential order of binding to the transporter; and (ii) ordered, which occurs if one of the substrates binds first to the transporter. These two types can be discriminated by analyzing the concentration independent constants Ks_1, Ks_2 and Ki_{S1}, Ki_{S2} (dissociation constant, respectively, of the ternary and binary transporter-substrate complexes) referred to the substrates (Cleland 1970). Constants were derived from the secondary plots obtained by re-plotting the values of the intercepts on the Y-axis or the slopes of the straight lines of Fig. 2, as function of the reciprocal substrate concentrations (insets of Fig. 2) (Indiveri et al. 2001). Concentration-independent Ks values were 20 mM for external Na^+, 20 μM for external glutamine and 1.8 mM for internal glutamine. The Ki_S values were 30 mM for external Na^+, 18 μM for external glutamine and 2.5 mM for internal glutamine, i.e., similar to the respective Ks values and fulfilling the relation $Ki_{S1} \times K_{S2} = K_{iS2} \times K_{S1}$. Taken together, these data demonstrate a random simultaneous mechanism in which the affinity of the transporter for one substrate is not influenced by the binding of the other substrates. It has been previously shown that besides glutamine also serine, asparagine, threonine are transported bidirectionally by hASCT2 while alanine is only inwardly transported (Pingitore et al. 2013). Km values on the external and internal side of the transporter were measured in the present work following the transport rate as dependence of the external or internal concentrations of each transported amino acid in exchange with glutamine (Table 1). A clear asymmetry of Km values

Table 1 Internal and external Km of hASCT2 for neutral amino acids

Substrate	Km (mM)	Km ex (μM)
Glutamine	1.8 ± 0.15	39 ± 3.9
Serine	6.6 ± 1.4	56 ± 12
Asparagine	1.6 ± 0.14	67 ± 5.1
Threonine	6.9 ± 0.21	36 ± 5.3
Alanine	Not transported	29 ± 2.2

The values reported are calculated according to Michaelis–Menten equation and are mean of 4 different experiments

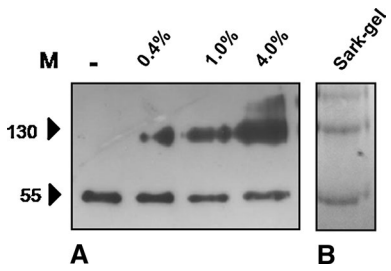

Fig. 3 Oligomeric state of hASCT2. In a, Immunoblot analysis of crosslinked protein. Purified, functional hASCT2 from *P. pastoris* has been treated with growing concentrations of formaldehyde, 0.4, 1 and 4 % as described in "Materials and methods". The western blot analysis has been performed using anti hASCT2 antibody 1:2000 dilution as described in "Materials and methods." In b, the purified, functional hASCT2 from *P. pastoris*, has been run on an electrophoresis gel under mild denaturing conditions, i.e., the gel, the running buffer and the sample buffer contained the mild denaturing detergent sarkosyl (1 %) instead of the denaturing SDS

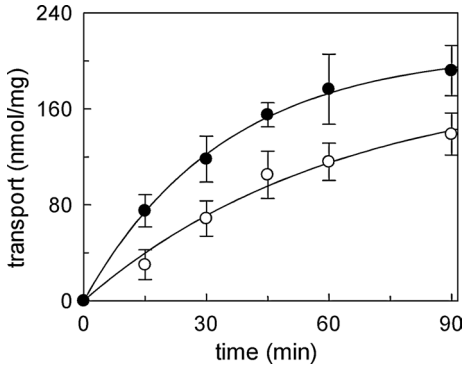

Fig. 4 Effect of membrane potential on the Na^+-glutamine$_{ex}$/glutamine$_{in}$ transport reaction. 50 μM [^{3}H]glutamine together with 50 mM Na-gluconate and 0.5 mM K-gluconate was added at time zero to proteoliposomes containing 50 mM K-gluconate in presence of valinomycin (*filled circle*) or ethanol (*unfilled circle*). The transport reaction was stopped at the indicated times, as described in "Materials and methods." The values are mean ± SD from three experiments

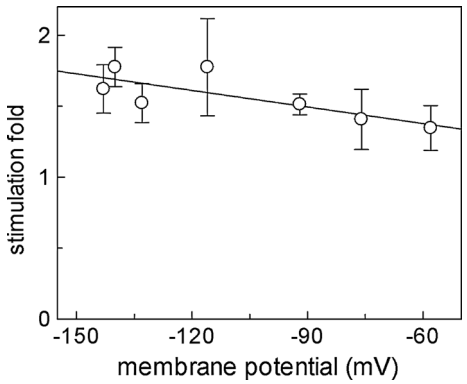

Fig. 5 Dependence of Na^+-glutamine$_{ex}$/glutamine$_{in}$ antiport rate on membrane potential values. 50 μM [^{3}H]glutamine together with 50 mM Na-gluconate was added at time zero to proteoliposomes containing 50 mM K-gluconate in presence of valinomycin or ethanol. The *X*-axis values are different membrane potential conditions derived from Nernst equation, imposed by varying external K-gluconate concentrations. The *Y*-axis values represent fold of stimulation of transport activity as ratio of valinomycin measured [^{3}H]glutamine uptake vs ethanol measured uptake. The transport reaction was stopped at 10 min, as described in "Materials and methods." The values are mean ± SD from three experiments

(see Table 1) for the various amino acids was observed. The Km values for the external site were similar for the different amino acids and lower than the corresponding internal values. The internal Km for glutamine (from Fig. 2) and asparagine were lower than those for serine and threonine (Table 1). The internal Km for alanine was not detectable; this correlated well with the lack of outwardly directed alanine transport (Pingitore et al. 2013).

The simultaneous transport mechanism implies binding sites for different substrates simultaneously present on the external and internal sides of the protein. This can be fulfilled by an oligomeric protein in which two (or more) monomers have the substrate binding site alternatively exposed on one of the two sides of the membrane (see discussion). The existence of oligomeric forms of hASCT2 was previously hypothesized (Pingitore et al. 2013). To verify this hypothesis, a cross-linking strategy was adopted. The purified functional protein was treated with different concentrations of formaldehyde and then analyzed by SDS-PAGE and immuno-blot. This analysis (Fig. 3a) revealed the formation of covalent oligomers which cannot be solved by SDS-PAGE, with a molecular mass almost double compared to the hASCT2 monomer. Moreover, the amount of cross-linked form depended on the formaldehyde concentration. To prove the specificity of formaldehyde reaction, the purified protein was run onto mild denaturing gel. Also in this case the presence of an oligomer with the same molecular mass of that found upon cross-linking, was observed (Fig. 3b). This data demonstrated that most of the protein is, at least, in a dimeric state.

Electrical properties of hASCT2 and regulation by Na^+

It was previously reported that hASCT2 is inactive in the absence of external Na^+ (Pingitore et al. 2013) indicating that the external Na^+ is essential for transport, in a concentration dependent fashion. In this work, the Na^+-coupled antiport reaction was studied in the presence of an inside negative potential. The membrane potential was obtained by imposing a K^+ outwardly directed gradient in proteoliposomes and adding valinomycin, a specific K^+ ionophore. It mediates efflux of K^+, generating a negative inside membrane potential. The time course of glutamine antiport was stimulated in the presence of membrane potential (Fig. 4). Under this condition, the transport rate, derived by interpolating the experimental data in a first-order rate equation, was doubled, being 6.1 nmol min^{-1} mg $protein^{-1}$ compared to 2.9 nmol min^{-1} mg $protein^{-1}$ in the absence of membrane potential. The substitution of Na-gluconate with NaCl or K-gluconate with KCl did not change the curve shapes, indicating that Cl^- is not involved in the transport reaction (not shown). When the transport stimulation was studied as dependence on the membrane potential, calculated on the basis of the Nernst equation (see "Materials and methods"), a linear behavior was observed (Fig. 5). The stimulation fold extrapolated from this graph at membrane potential equal to 0, was very close to 1, i.e., absence of stimulation (not shown). However, the stimulation was lower than expected. Some properties of the transporter and/or of the membrane may contribute to this discrepancy: (1) an unspecific ion conductance overlapping the transport activity as previously described for ASCT2 (Broer et al. 2000), (2) a small permeability of the liposomal membrane to protons, which may reduce the potential to some extent. On the basis of these results it can be hypothesized that Na^+ is transported from outside to inside and not vice versa with accumulation of positive charges in the intra-liposomal compartment. In the case of hASCT2, no Na^+-glutamine cotransport is detectable in the absence of intra-liposomal substrate (Pingitore et al. 2013) even in the presence of membrane potential (not shown).

As previously reported, the intra-liposomal (intracellular) Na^+ slightly stimulated the glutamine/glutamine antiport (Pingitore et al. 2013). To gain further insights in this aspect, the dependence of transport activity on intra-liposomal Na^+, in the absence or presence of membrane potential, was studied. The results showed a nearly hyperbolic behavior in the absence of potential, reaching a plateau at concentrations of Na^+ above 20 mM (Fig. 6). Very interestingly, in the presence of membrane potential an evident change of the shape of the Na^+ dependence curve was observed, with a maximal transport activity at 10 mM internal Na^+. Noteworthy, with no internal Na^+, the activity in the presence of membrane potential was higher than in its absence, confirming that the electrogenicity derives from external Na^+. At higher intra-liposomal Na^+ concentration, the transport activity decreased. However, the membrane potential still stimulated the transport at 50 mM Na^+ (equal external and internal concentrations). These data suggest that the stimulatory effect of Na^+ from the internal side is not due to transport but to an allosteric/binding effect. To evaluate possible influence of internal Na^+ on kinetic parameters, Km for glutamine and Vmax were measured in the presence or absence of 10 mM internal Na^+. No variation of Km for external and internal glutamine was found, while Vmax was increased in the presence of Na^+ (not shown).

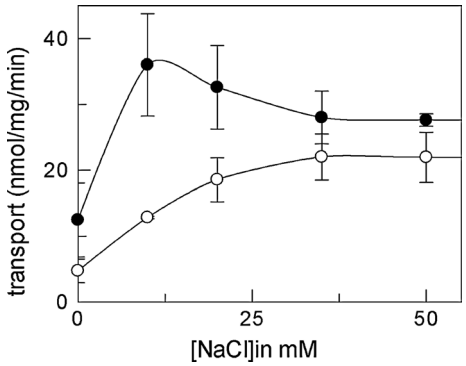

Fig. 6 Dependence of Na^+-glutamine$_{ex}$/glutamine$_{in}$ antiport rate on internal Na^+. 50 µM [^{3}H]glutamine together with 50 mM Na-gluconate and 0.5 mM K-gluconate was added at time zero to proteoliposomes containing NaCl at the indicated concentrations and 50 mM K-gluconate in presence of valinomycin (*filled circle*) or ethanol (*unfilled circle*). To balance osmolarity, deriving from NaCl, increasing sucrose concentrations (from 100 to 0 mM) were added to proteoliposomes. The transport reaction was stopped at 10 min, as described in "Materials and methods". The values are mean ± SD from three experiments

Reconstitution of hASCT2 from HeLa cells and effect of deglycosylation

To confirm the suitability of the recombinant protein for functional studies, the endogenous hASCT2 was extracted from HeLa cells, where it was significantly expressed (Fig. 7a), and then reconstituted in liposomes. Immuno-blot showed a molecular mass of hASCT2 higher than the theoretical one, probably due to the presence of glycosylation moiety(ies). The different bands can be explained by the presence of several glycosylated forms. However, at this stage, we cannot exclude that some glycosyl moieties may be lost during protein extraction. After treatment by glycosydase, a lower molecular mass of ASCT2 was found, corresponding to the apparent molecular mass of the protein obtained by over-expression in *P. pastoris* (Pingitore et al. 2013).

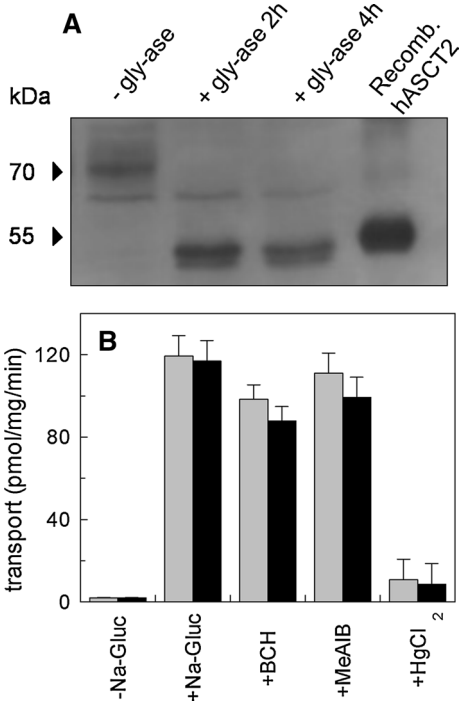

Fig. 7 Deglycosylation and transport function of hASCT2 extracted from HeLa cells. **a** hASCT2 from HeLa cells before and after deglycosylation treatment (according to manufacturers' conditions). *Lane 1*: 10 µg of total lysate without glycosidase (gly-ase); *lane 2* and *3*: 10 µg of total lysate upon 2 h and 4 h of glycosidase treatment (+ gly-ase), respectively. Lane 4: 1 µg of purified hASCT2 overexpressed in *P. pastoris*. Arrows indicate the specific hASCT2 protein band (using anti-hASCT2 1:2000) and the shift of molecular mass upon deglycosylation treatment. **b** Uptake of [^{3}H]glutamine in Proteoliposomes reconstituted with hASCT2 extracted from HeLa cells, as described in "Materials and methods," before (*dark gray*) and after (*light gray*) 2 h deglycosylation treatment. The uptake of 50 µM [^{3}H]glutamine has been measured in absence or presence of external 50 mM Na-gluconate or in presence of 10 mM BCH or 10 mM MeAIB or 10 µM $HgCl_2$. The transport reaction was stopped after 30 min, as described in "Materials and methods." The values are mean ± SD from three experiments

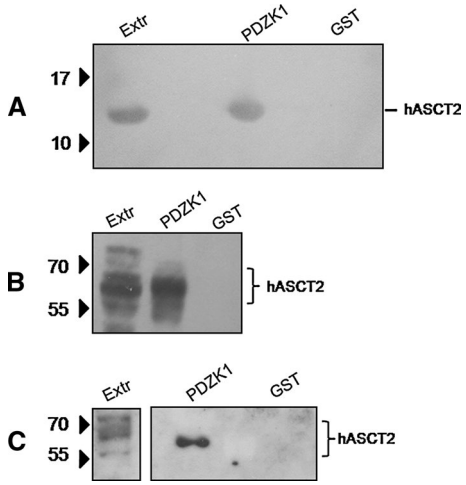

Fig. 8 Binding of PDZK1 to C-terminal peptide and native hASCT2. **a** the C-terminal region of hASCT2 (aa 447-541) was expressed in *E. coli* cells as His-recombinant protein. Bacterial lysate was incubated with PDZK1-GST bound on Sepharose beads or GST alone as a control. The fraction of ASCT2 retained on the column was revealed by POD-conjugated, anti-His antibody as described in "Materials and methods." **b** HeLa cell total extract over- expressing hASCT2 was incubated with PDZK1-GST or GST alone. HeLa cells were seeded onto 10 cm^2 plate and were transfected with 3 µg of ASCT2-pCDNA3 with Lipofectamine according to manufacturers' conditions. **c** HeLa cell total extract expressing endogenous ASCT2 was incubated with PDZK1-GST or GST alone. The binding was revealed by anti-ASCT2 antibody (1:2000) as described in "Materials and methods"

The ASCT2 extracted from HeLa was then reconstituted in proteoliposomes. It was identified by testing the main functional properties, i.e., Na^+ dependence, antiport mode of transport, inhibition by the ASCT2 inhibitor $HgCl_2$ and insensitivity to MeAIB or BCH, i.e., specific inhibitors of the alternative glutamine transporters System A and L, respectively (Fig. 7b; Pingitore et al. 2013). Noteworthy, after cleavage of the glycosyl moieties, the protein function was still strictly dependent on the presence of external Na^+ and internal glutamine. The same results were obtained in the presence of intra liposomal serine, asparagine or threonine (not shown). Moreover, the strong inhibition exerted by $HgCl_2$, as well as the lack of inhibition by MeAIB or BCH demonstrated that the transporter maintained the same features of the glycosylated protein and of the recombinant protein. Therefore, the carbohydrate moieties were not involved in transport function (Fig. 7b).

hASCT2-PDZK1 interaction

The evidence that ASCT2 plays important roles in complex intracellular pathways suggested that interactions with specific modulators could occur. Interaction of hASCT2 with scaffold proteins was predicted by the presence, in its primary structure, of a class I consensus sequence recognized by PDZ domains: $X[T/S]X\Phi_{COOH}$, where X is any residue and Φ is a hydrophobic one (Tonikian et al. 2008). A recombinant peptide corresponding to the cytosolic, C-terminal fragment of the protein (aa 447-541) was produced in *E.coli* and tested for its ability to recognize PDZ proteins. Noteworthy, PDZK1 is a scaffold protein constituted of four PDZ domains, that has been described to regulate several membrane transporters belonging to the SLC families (Kato et al. 2005; Hu et al. 2009). A GST pull-down assay was performed to verify if PDZK1 could bind to the C-terminal of hASCT2. As shown in Fig. 8a, a specific interaction of the peptide with the recombinant PDZK1 was detected by anti-His antibody against the His-tagged

hASCT2 peptide produced in *E.coli*. The molecular mass of the peptide recognized by the anti-His antibody, well corresponded to the theoretical molecular mass of the recombinant 6-His-tagged peptide, i.e., 14189 Da. To verify that also the full-length hASCT2 could bind to PDZK1, the protein was over-expressed in HeLa cells and the same pull-down experiment was performed (Fig 8b). The definitive proof of interaction with PDZK1 protein came from pull-down with the endogenous ASCT2 from HeLa cells. Again a specific reaction was observed after affinity purification of HeLa extract on PDZK1- resin and staining with the anti-hASCT2 antibody (Fig. 8c). The different bands detected in the total extract corresponded to different glycosylated products of ASCT2 as above described.

Discussion

In this work, the human ASCT2 glutamine/neutral amino acid transporter was characterized for the first time in an isolated environment, thanks to the availability of the functional recombinant protein and the proteoliposome tool. This experimental system gives the main advantage of studying uniquely the features of the human transport protein inserted in the bilayer with the same orientation of cell membrane (Fig. 1; Pingitore et al. 2013) in absence of any interferences from other transporters or enzymes. Indeed using the detergent removal reconstitution procedure, hASCT2 sided proteoliposomes were obtained, as it was previously described for other transporters (Flugge 1992; Palmieri et al. 1995; Scalise et al. 2013). The still unknown kinetic mechanism of hASCT2 was assessed. A random simultaneous mechanism was revealed with no preference of binding order for the substrates. This is one of the two known mechanisms for co-transporters in which slippage is negligible, i.e., obligatory co-transporters (Stein 1989) like hASCT2 which exhibits no activity in the absence of external Na^+ (Pingitore et al. 2013). Moreover, ASCT2 has an unusual coupling of co-transport to counter exchange of internal amino acids. This mechanism is indeed performed by the overall transport reaction (Fig. 2). This feature is somewhat similar to the rat kidney isoform in proteoliposomes, for which, however, small variations of half-saturation constants were found depending on the co-substrate concentration, in line with the significant local differences in the amino acid sequences between the two proteins (see below) or the difference in regulation by intracellular ATP (Oppedisano et al. 2007; Pingitore et al. 2013). The simultaneous mechanism, which explains the transport reaction by a well-defined model, can be interpreted in the light of the quaternary structure of the transporter. The functional hASCT2 transporter is likely to be constituted by, at least, two subunits as demonstrated by the shift towards a higher molecular mass of the protein after covalent cross-linking, similarly to other transporters (Yernool et al. 2004). The experimental data on the sidedness, the asymmetry in Km values and the requirement of external Na^+ (see Results and Pingitore et al. 2013) indicate that each monomer should be inserted into the membrane with the same orientation. Then, each subunit may give rise to a transport cycle in which the simultaneous translocation of different substrates occurs in opposite direction. The model of an oligomeric state of hASCT2 traces the one recently described for elevator type transporters (Lee et al. 2013). Also for the rat isoform an oligomeric functional state has been hypothesized by several authors, on the basis of homology with the tridimensional structure of Glpth from *P. horikoshii* (Oppedisano et al. 2010; Albers et al. 2012; Zander et al. 2013). The kinetic data gave rise to important speculation on the role of hASCT2 both in physiological and pathological contexts. The lower affinity for hydroxyl amino acids on the internal side indicates that the two molecules would be preferentially taken up according to their plasmatic concentration (Cynober 2002). This is also in line with the higher external affinity of the transporter for threonine and serine. The finding is interesting also from a pathological point of view, since serine, besides glutamine, is important in cancer cells for maintaining the redox homeostasis necessary for their survival. Noteworthy, it has been recently reported that serine starvation induces increased ROS production in some cancers with consequent cell cycle arrest (Maddocks et al. 2013). Furthermore, in cancer cells, where ASCT2 is over-expressed and the request of glutamine is higher than normal, the reaction mediated by ASCT2 should lead mainly to glutamine uptake in exchange with other amino acids with smaller side chains allowing net import of reduced carbon atoms to fulfill energetic purposes ("Introduction"; Ganapathy et al. 2009).

Another important aspect dealt with in this work is the electrogenic nature of the Na^+-coupled amino acid antiport. The described data are in favor of inward transport of one Na^+ per glutamine with consequent electrogenicity of the transport reaction. However, we cannot completely exclude that more than one Na^+ may be involved in inward transport, if the binding of ions is independent from each other. The suggested mechanism, which does not represent a definitive proof, is compatible with the recent data obtained in cell systems on the rat ASCT2 even though with some differences (Zander et al. 2013), which are justified by the structural diversity of the two isoforms. Indeed, aligning the rat and the human transporters, an overall identity of 79 % is found, which is not as high as the identity among other membrane transporters of the two organisms (Broer et al. 1999; Oppedisano et al. 2011; Indiveri et al. 2013). This relatively low identity accounts for some functional differences like the broader substrate specificity of

hASCT2 compared to rat isoform or the ability of evoking currents of hASCT2 compared to electroneutrality of the rat isoform (Broer et al. 1999). Other structural differences arise from this comparison: rat isoform has 16 Cys while human only 8; moreover, only the rat isoform harbors a CXXC motif responsible for the very strong interaction with heavy metals (Oppedisano et al. 2010). This motif is located in a stretch of 31 amino acids (from 239 to 270) in which the local identity between rat and human is only 12 % (not shown). However, knowledge of the functional role of this stretch requires further investigation.

Interestingly, proteoliposomes allowed us to investigate the role of internal Na^+. It plays a regulatory function under physiological conditions since the best activating concentration of Na^+ corresponds to its average intracellular concentration (Fleysher et al. 2013). On the basis of the effect of internal Na^+ on V_{max} but not on Km for glutamine "Results", it can be inferred that the stimulation may be caused by the increased coupling between the two subunits or by stabilization of the transporter transition state. Taken together, the experimental data allowed to conclude that the mechanism of transport is complex and finely regulated: the driving force is, indeed, constituted by the antiport component (guided by different amino acid concentrations across membrane in vivo), the inwardly directed Na^+ concentration gradient and, at lower extent, the electrical component.

Nearly nothing is known about regulation of ASCT2 either by post-translational modifications or interactions with other proteins. We have demonstrated here that the glycosyl moieties of ASCT2 have no role in transport function, thus validating the suitability of the recombinant protein for functional characterization. This post-translational modification, has been suggested as not essential for function of other transporters studied in cell systems (Vickers et al. 1999; Quick and Wright 2002; Keller et al. 2008; Filippo et al. 2011) even though a direct proof was not available. Thus, the experiments performed in proteoliposomes on ASCT2 may suggest a possible general rule for membrane transporters. These preliminary results open interesting perspectives for investigating the role of glycosylation and of other potential post-translational modifications of ASCT2. On the basis of proteomics, indeed, PhosphoSite database (http://www.phosphosite.org/homeAction.do) counts 11 phosphorylation and 7 ubiquitination sites observed in the human protein by mass spectrometry analysis. The protein modification possibly occurring in these sites might be involved in the control of hASCT2 function acting, on the one hand, on the protein expression/delivery in plasma membrane (Avissar et al. 2008), on the other hand, on its degradation.

On the basis of the described results, the recombinant hASCT2, which functions as the native protein, is useful for large-scale screening of inhibitors, as potential anticancer drugs. The proteoliposomes tool, in fact, has already proved suitable for such studies (Pochini et al. 2013, 2014). Lastly, in this paper, an interaction between ASCT2 and a scaffold protein has been shown, for the first time. The analysis of the intracellular C-terminal of hASCT2 showed that it contains a class I PDZ binding motif. The PDZ domains are composed by 80–90 amino acids and represent the most abundant interaction domains encoded in the human genome. The PDZ modules are highly conserved across evolution and are involved in several cellular pathways under both physiological and pathological conditions. Interestingly, several membrane transporters, involved in drug and nutrient disposition are regulated by PDZ proteins such as PDZK1, PDZK2, NHERF1 and NHERF2 (Sugiura et al. 2011). The interaction with these proteins seems to be involved in sorting and membrane stabilization of the transporters. In the case of hASCT2, a strong interaction between PDZK1 and the C-terminal of the protein has been reported here. The results are in line with the co-expression of the two proteins in different normal and neoplastic tissues (http://www.proteinatlas.org/). These findings correlate well with the intracellular localization of the C-terminal of hASCT2. (Pingitore et al. 2013; Fig. 1). These results represent the basis for identifying the PDZ domain, among the four present in PDZK1, directly involved in the interaction with ASCT2. This will shed light on the cell pathway involved in ASCT2 regulation, since each PDZ domain can activate different intracellular metabolic cascades. A further regulatory role may be played by two potential phosphorylation sites in the C-terminal motif (SEKESVM), which can change the binding specificity of the sequence toward PDZK1 (Dephoure et al. 2008; Thingholm et al. 2008). From all the data here described, it appears that the function of hASCT2 can be modulated at different levels, fulfilling the pivotal role of mediator of amino acid signaling and homeostasis in physiological conditions. Moreover, the suitability of the proteoliposome model for inhibitor's screening opens important application perspectives, since ASCT2 is a well-known player in cancer development and progression.

Acknowledgments This work was supported by funds from: Programma Operativo Nazionale [01_00937]-MIUR "Modelli sperimentali biotecnologici integrati per lo sviluppo e la selezione di molecole di interesse per la salute dell'uomo" to CI. The authors are grateful to Dr. Jean Jimenez for language revision.

Conflict of interest The authors declare that they have no conflict of interest.

References

Adeva MM, Souto G, Blanco N, Donapetry C (2012) Ammonium metabolism in humans Metabolism 61:1495–1511 doi:10.1016/j.metabol.2012.07.007

Shimizu K et al (2014) ASC amino-acid transporter 2 (ASCT2) as a novel prognostic marker in non-small cell lung cancer. British J Cancer. doi:10.1038/bjc.2014.88

Albers T, Marsiglia W, Thomas T, Gameiro A, Grewer C (2012) Defining substrate and blocker activity of alanine-serine-cysteine transporter 2 (ASCT2) Ligands with Novel Serine Analogs. Mol Pharmacol 81:356–365. doi:10.1124/mol.111.075648

Avissar NE, Sax HC, Toia L (2008) In human entrocytes, GLN transport and ASCT2 surface expression induced by short-term EGF are MAPK, PI3 K, and Rho-dependent. Dig Dis Sci 53:2113–2125

Bode BP (2001) Recent molecular advances in mammalian glutamine transport. The Journal of nutrition 131:2475S–2485S (discussion 2486S-2477S)

Broer S (2011) Targeting tumour cells at the entrance. Biochem J 439:e1–e2. doi:10.1042/BJ20111484

Broer A, Brookes N, Ganapathy V, Dimmer KS, Wagner CA, Lang F, Broer S (1999) The astroglial ASCT2 amino acid transporter as a mediator of glutamine efflux. J Neurochem 73:2184–2194

Broer A, Wagner C, Lang F, Broer S (2000) Neutral amino acid transporter ASCT2 displays substrate-induced Na^+ exchange and a substrate-gated anion conductance. Biochem J 346(Pt 3):705–710

Cleland WW (1970) The enzymes, kinetics and mechanism (vol II). Academic Press, London

Cynober LA (2002) Plasma amino acid levels with a note on membrane transport: characteristics, regulation, and metabolic significance. Nutrition 18:761–766

Dephoure N, Zhou C, Villen J, Beausoleil SA, Bakalarski CE, Elledge SJ, Gygi SP (2008) A quantitative atlas of mitotic phosphorylation. Proc Natl Acad Sci 105:10762–10767. doi:10.1073/pnas.0805139105

Filippo CA, Ardon O, Longo N (2011) Glycosylation of the OCTN2 carnitine transporter: study of natural mutations identified in patients with primary carnitine deficiency. Biochim Biophys Acta 1812:312–320. doi:10.1016/j.bbadis.2010.11.007

Fleysher L, Oesingmann N, Brown R, Sodickson DK, Wiggins GC, Inglese M (2013) Noninvasive quantification of intracellular sodium in human brain using ultrahigh-field MRI. NMR Biomed 26:9–19. doi:10.1002/nbm.2813

Flugge UI (1992) Reaction mechanism and asymmetric orientation of the reconstituted chloroplast phosphate translocator. Biochim Biophys Acta 1110:112–118

Fuchs BC, Bode BP (2005) Amino acid transporters ASCT2 and LAT1 in cancer: partners in crime? Semin Cancer Biol 15:254–266. doi:10.1016/j.semcancer.2005.04.005

Fuchs BC, Finger RE, Onan MC, Bode BP (2007) ASCT2 silencing regulates mammalian target-of-rapamycin growth and survival signaling in human hepatoma cells. Am J Cell Physiol 293:C55–C63. doi:10.1152/ajpcell.00330.2006

Ganapathy V, Thangaraju M, Prasad PD (2009) Nutrient transporters in cancer: relevance to Warburg hypothesis and beyond. Pharmacol Ther 121:29–40. doi:10.1016/j.pharmthera.2008.09.005

Giancaspero TA et al (2013) FAD synthesis and degradation in the nucleus create a local flavin cofactor pool. J Biol Chem 288:29069–29080. doi:10.1074/jbc.M113.500066

Hu S et al (2009) Systematic analysis of a simple adaptor protein PDZK1: ligand identification, interaction and functional prediction of complex. Cell Physiol Biochem 24:231–242. doi:10.1159/000233258

Indiveri C, Dierks T, Kramer R, Palmieri F (1991) Reaction mechanism of the reconstituted oxoglutarate carrier from bovine heart mitochondria. Eur J Biochem 198:339–347

Indiveri C, Tonazzi A, De Palma A, Palmieri F (2001) Kinetic mechanism of antiports catalyzed by reconstituted ornithine/citrulline carrier from rat liver mitochondria. Biochim Biophys Acta 1503:303–313

Indiveri C, Galluccio M, Scalise M, Pochini L (2013) Strategies of bacterial over expression of membrane transporters relevant in human health: the successful case of the three members of OCTN subfamily. Mol Biotechnol 54:724–736. doi:10.1007/s12033-012-9586-8

Kato Y, Sai Y, Yoshida K, Watanabe C, Hirata T, Tsuji A (2005) PDZK1 directly regulates the function of organic cation/carnitine transporter OCTN2. Mol Pharmacol 67:734–743. doi:10.1124/mol.104.002212

Keller T, Schwarz D, Bernhard F, Dotsch V, Hunte C, Gorboulev V, Koepsell H (2008) Cell free expression and functional reconstitution of eukaryotic drug transporters. Biochemistry 47:4552–4564. doi:10.1021/bi800060w

Lee C et al (2013) A two-domain elevator mechanism for sodium/proton antiport. Nature 501:573–577. doi:10.1038/nature12484

Maddocks OD, Berkers CR, Mason SM, Zheng L, Blyth K, Gottlieb E, Vousden KH (2013) Serine starvation induces stress and p53-dependent metabolic remodelling in cancer cells. Nature 493:542–546. doi:10.1038/nature11743

Nicklin P et al (2009) Bidirectional transport of amino acids regulates mTOR and autophagy. Cell 136:521–534. doi:10.1016/j.cell.2008.11.044

Oppedisano F, Indiveri C (2008) Reconstitution into liposomes of the B degrees -like glutamine-neutral amino acid transporter from renal cell plasma membrane. Biochim Biophys Acta 1778:2258–2265. doi:10.1016/j.bbamem.2008.05.01

Oppedisano F, Pochini L, Galluccio M, Cavarelli M, Indiveri C (2004) Reconstitution into liposomes of the glutamine/amino acid transporter from renal cell plasma membrane: functional characterization, kinetics and activation by nucleotides. Biochim Biophys Acta 1667:122–131. doi:10.1016/j.bbamem.2004.09.007

Oppedisano F, Pochini L, Galluccio M, Indiveri C (2007) The glutamine/amino acid transporter (ASCT2) reconstituted in liposomes: transport mechanism, regulation by ATP and characterization of the glutamine/glutamate antiport. Biochim Biophys Acta 1768:291–298. doi:10.1016/j.bbamem.2006.09.002

Oppedisano F, Galluccio M, Indiveri C (2010) Inactivation by Hg2 + and methylmercury of the glutamine/amino acid transporter (ASCT2) reconstituted in liposomes: prediction of the involvement of a CXXC motif by homology modelling. Biochem Pharmacol 80:1266–1273. doi:10.1016/j.bcp.2010.06.032

Oppedisano F, Pochini L, Broer S, Indiveri C (2011) The B degrees AT1 amino acid transporter from rat kidney reconstituted in liposomes: kinetics and inactivation by methylmercury. Biochim Biophys Acta 1808:2551–2558. doi:10.1016/j.bbamem.2011.05.011

Oppedisano F et al (2012) Inactivation of the glutamine/amino acid transporter ASCT2 by 1,2,3-dithiazoles: proteoliposomes as a tool to gain insights in the molecular mechanism of action and of antitumor activity. Toxicol Appl Pharmacol 265:93–102. doi:10.1016/j.taap.2012.09.011

Palmieri F, Indiveri C, Bisaccia F, Iacobazzi V (1995) Mitochondrial metabolite carrier proteins: purification, reconstitution, and transport studies. Methods Enzymol 260:349–369

Pingitore P, Pochini L, Scalise M, Galluccio M, Hedfalk K, Indiveri C (2013) Large scale production of the active human ASCT2 (SLC1A5) transporter in Pichia pastoris–functional and kinetic asymmetry revealed in proteoliposomes. Biochim Biophys Acta 1828:2238–2246. doi:10.1016/j.bbamem.2013.05.034

Pochini L, Scalise M, Galluccio M, Indiveri C (2012) Regulation by physiological cations of acetylcholine transport mediated by human OCTN1 (SLC22A4). Implications in the non-neuronal cholinergic system. Life Sci 91:1013–1016. doi:10.1016/j.lfs.2012.04.027

Pochini L, Scalise M, Galluccio M, Indiveri C (2013) OCTN cation transporters in health and disease: role as drug targets and assay development. J Biomol Screen 18:851–867. doi:10.1177/1087057113493006

Quick M, Wright EM (2002) Employing Escherichia coli to functionally express, purify, and characterize a human transporter. Proc Natl Acad Sci USA 99:8597–8601. doi:10.1073/pnas.132266599

Scalise M, Pochini L, Giangregorio N, Tonazzi A, Indiveri C (2013) Proteoliposomes as tool for assaying membrane transporter functions and interactions with xenobiotics. Pharmaceutics 5:472–497. doi:10.3390/pharmaceutics5030472

Stein WD (1989) Kinetics of transport: analyzing, testing, and characterizing models using kinetic approaches. Methods Enzymol 171:23–62

Sugiura T, Shimizu T, Kijima A, Minakata S, Kato Y (2011) PDZ adaptors: their regulation of epithelial transporters and involvement in human diseases. J Pharm Sci 100:3620–3635. doi:10.1002/jps.22575

Thingholm TE, Larsen MR, Ingrell CR, Kassem M, Jensen ON (2008) TiO(2)-based phosphoproteomic analysis of the plasma membrane and the effects of phosphatase inhibitor treatment. J Proteome Res 7:3304–3313. doi:10.1021/pr800099y

Tonikian R et al (2008) A specificity map for the PDZ domain family. PLoS Biol 6:e239. doi:10.1371/journal.pbio.0060239

Torres-Zamorano V, Leibach FH, Ganapathy V (1998) Sodium-dependent homo- and hetero-exchange of neutral amino acids mediated by the amino acid transporter ATB degree. Biochem Biophys Res Comm 245:824–829

Utsunomiya-Tate N, Endou H, Kanai Y (1996) Cloning and functional characterization of a system ASC-like Na + -dependent neutral amino acid transporter. J Biol Chem 271:14883–14890

Vickers MF, Mani RS, Sundaram M, Hogue DL, Young JD, Baldwin SA, Cass CE (1999) Functional production and reconstitution of the human equilibrative nucleoside transporter (hENT1) in Saccharomyces cerevisiae. Interaction of inhibitors of nucleoside transport with recombinant hENT1 and a glycosylation-defective derivative (hENT1/N48Q). Biochem J 339(Pt 1):21–32

Yernool D, Boudker O, Jin Y, Gouaux E (2004) Structure of a glutamate transporter homologue from Pyrococcus horikoshii. Nature 431:811–818. doi:10.1038/nature03018

Zander CB, Albers T, Grewer C (2013) Voltage-dependent processes in the electroneutral amino acid exchanger ASCT2. J Gen Physiol 141:659–672. doi:10.1085/jgp.201210948